

# Field-based Parameterisation of Cardiac Muscle Structure from Diffusion Tensors

Bianca Freytag, Vicky Wang, Richard Christie, Alexander Wilson, Gregory Sands, Ian LeGrice, Alistair Young, Martyn Nash

## Background

Diffusion tensor MRI exploits Brownian motion of water molecules within soft tissue (e.g. brain, heart) to determine local anisotropic diffusion<sup>1</sup>. The direction of maximum water diffusion, represented by the primary eigenvector of the derived diffusion tensor, has been found to correlate well with the local histologically-measured myofibre orientation<sup>2,3</sup>.

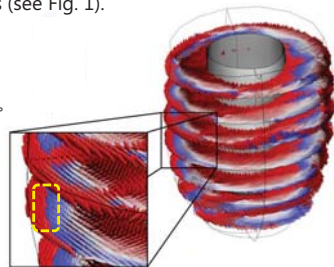
Fibre orientations of the heart, derived from diffusion tensors, are often represented as fibre angles with respect to the short-axis plane of the heart.

There are two main disadvantages in using the primary eigenvector to calculate fibre orientations:

- i. Water diffuses equally in opposite directions but the primary eigenvector arbitrarily represents just one of these directions (see Fig. 1).



Fig. 1: Primary eigenvectors colour-coded by fibre angles



- ii. In regions of apparent near-isotropic diffusion, indicated by a low fractional anisotropy (FA), the eigenvector may not reliably represent the local tissue microstructure (see Fig. 2).

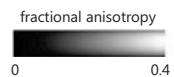
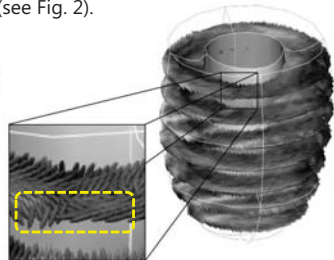


Fig. 2: Primary eigenvectors colour-coded by fractional anisotropy



## Motivation

We present a workflow for model-based parameterisation of myocardial fibre fields directly from the diffusion tensors to circumvent the above disadvantages.

## Method

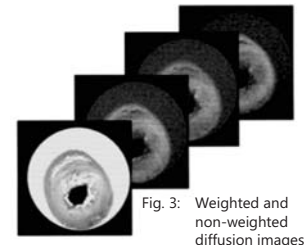


Fig. 3: Weighted and non-weighted diffusion images

### Diffusion tensor calculation

From the non-diffusion weighted signals ( $S_0$ ) and the diffusion weighted signals ( $S_k$ ) captured in non-collinear directions (i.e.  $k = 1..30$ ), a symmetric diffusion tensor, denoted  $D_{ij}$ , was estimated for each voxel by solving the logarithm of the diffusion equation proposed by Basser et al.<sup>1</sup>

$$\log(S_k) = \log(S_0) - b \sum_{i=1}^3 \sum_{j=1}^3 (Q_k)_{ij} D_{ij}$$

### Image segmentation

Endocardial and epicardial surfaces of the LV were manually segmented from the non-diffusion images using MATLAB.

The contours were transformed to the cardiac coordinate system defined by three landmark points (centroids of the LV base, LV apex, and RV base) selected from the non-diffusion weighted image.

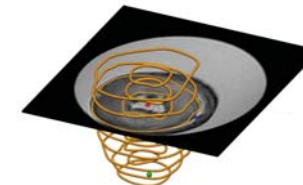


Fig. 4: Segmented surfaces and landmark points

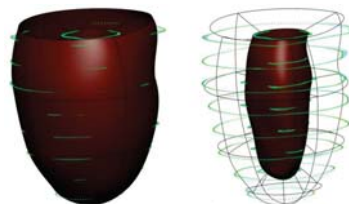


Fig. 5: Fitted FE LV model

### LV FE geometric model construction

A 16-element tricubic-Hermite FE model was customised to the surface contours obtained from Step 2. The endocardial and epicardial surfaces of the model were fitted to best match the corresponding surface data.

### Field-based parameterisation of LV fibre orientation

The FE fibre angle field was initialised by setting the fibre angles to  $\theta_n = +60^\circ$  (endocardial nodes), and  $\theta_n = -70^\circ$  (epicardial nodes). Imbrication angles ( $\varphi_n$ ) of all nodes were set to be  $0^\circ$ . These angles were interpolated over the FE model with tricubic-Hermite basis functions.

For each voxel ( $v$ ) the FE local coordinates within the LV geometric model were determined. At those locations the myofibre orientation  $f_v$ , defined by Euler angle rotations (using interpolated  $\theta$  and  $\varphi$ ), was computed.

An objective function was constructed to maximise the local diffusion direction  $f_v$ , by modifying the nodal fibre parameters ( $\theta_v$  and  $\varphi_v$ ).

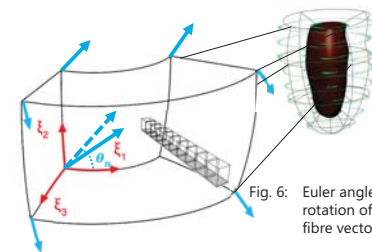


Fig. 6: Euler angle rotation of fibre vectors

$$F = \sum_{v=1}^N (f_v^i) \text{ where } f_v^i = f_{i,v} D_{ij,v} f_{j,v} \text{ summed over } i, j$$

$v = 1..N$  is the number of voxels

## Results

The fitted fibre angle field showed a smooth transmural variation as expected (see Fig. 7).

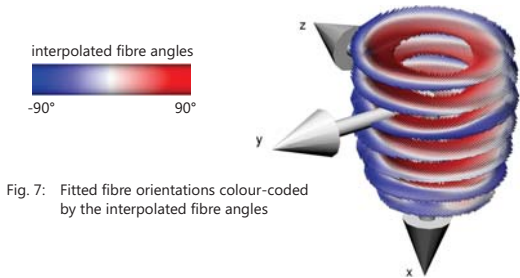


Fig. 7: Fitted fibre orientations colour-coded by the interpolated fibre angles

In regions with high FA values, the fitted fibre orientations correlated well with the primary eigenvectors as indicated by the dot product map shown in Fig. 8 (a). This correlation was low in regions with low FA as highlighted in Fig. 8 (b).

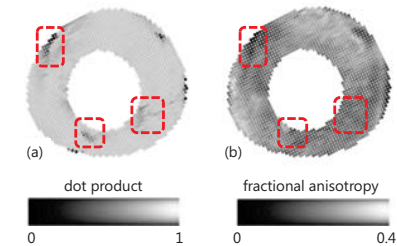


Fig. 8: (a) Map of dot-products between interpolated fibre vectors and primary eigenvectors of  $D$ . (b) Map of FA values for the same mid-ventricular slice.

## Conclusion

This novel method to construct a model-based myocardial fibre field does not need to compute eigenvectors or FA values and circumvents issues associated with phase-unwrapping of eigenvectors prior to fibre fitting. It also helps to ensure that the interpolated fibre angles in regions with high FA are better representations of the diffusion tensors.

The workflow could be adapted to construct fibre fields using *in vivo* cardiac imaging data and associated geometric FE models for individualised analyses of heart mechanics.

- Basser, P.J., Mattiello, J., LeBihan, D.: Estimation of the effective self-diffusion tensor from the NMR spin echo. *Journal of Magnetic Resonance, Series B* 103, 247-254 (1994)
- Hsu, E.W., Muzikant, A.L., Matulevicius, S.A., Penland, R.C., Henriquez, C.S.: Magnetic resonance myocardial fiber-orientation mapping with direct histological correlation. *American Journal of Physiology* 275, H1627-1634 (1998)
- Scollan, D.F., Holmes, A., Winslow, R.L., Forder, J.: Histological validation of myocardial microstructure obtained from diffusion tensor magnetic resonance imaging. *American Journal of Physiology* 275(6 Pt. 2), H2308-2318 (1998)